Two-Dimensional Penning Ionization Electron Spectroscopy of HCl with He*(2^3S) Atom

Kohei Imura,† Naoki Kishimoto, and Koichi Ohno*

Department of Chemistry, Graduate School of Science, Tohoku University, Aramaki, Aoba-ku, Sendai 980-8578, Japan

Received: November 30, 2001; In Final Form: February 13, 2002

Penning ionization of HCl upon collision with metastable He*(2^3S) atoms was studied by two-dimensional (collision-energy/electron energy resolved) Penning ionization electron spectroscopy and by classical trajectory calculations. Collision energy resolved studies enable us to obtain important information about stereo dynamical aspects on this reaction; sideways approaches of the He* atoms on H−Cl molecular axis play a dominant role in the ionization event for producing $HCl^+(X\ ^2\Pi_i, v' = 0, 1)$, and glancing collision is one of the dominant trajectories of the He* atoms to produce $HCl^+(A, ^2\Sigma^+)$. It was also found that the formation of vibrationally excited $HCl^+(X\ ^2\Pi_i, v' > 1)$ through the unidentified HCl** Rydberg state was influenced by a strong attractive interaction, whereas the formation of the HCl** Rydberg state, dissociating to H(1s) and autoionizing Cl**($^1D_2$ *nl*) atoms, was found to be affected by a repulsive interaction around the Cl end of the HCl molecule.

I. Introduction

The reaction of metastable rare gas atoms with molecules has been of long-term interest, because of the variety of possible reaction channels involved. Among these, one of the most fundamental processes for chemiionization known as Penning ionization[1] has been widely studied in recent years.[2−5] Penning ionization of HCl with the metastable He*(2^3S) has been the focus of attention of numerous investigations by utilizing the Penning ionization electron spectroscopic (PIES)[6−11] and Penning ionization optical spectroscopic (PIOS)[12−17] techniques. PIES reveals the state distribution in which the molecular ion is formed, whereas PIOS probes the ions after the dissociation of the interacting reactants. Therefore, the nascent vibronic distributions of the ions may be different, if the initial distribution is perturbed in the collision complex. Richardson et al.[12,13] reported the non-Franck−Condon vibrational state distributions in the $HCl^+(A\ ^2\Sigma^+)$ state as nonvertical processes by using the PIOS. This study prompted several PIES studies with an aim on determining the nascent state distribution in the $HCl^+(A\ ^2\Sigma^+)$. The PIES studies reported,[6−10] basically, identical vibrational state distributions found in the He I ultraviolet photoelectron spectrum (UPS). Several possibilities have been discussed to explain the difference between the PIOS and PIES studies.

More recently, a high resolution and detailed PIES study reported by Yencha et al.[11] indicates very interesting features in the Penning ionization of HCl with He*(2^3S) and He*(2^1S) atoms. Although $HCl^+(X\ ^2\Pi_i)$ and $HCl^+(A\ ^2\Sigma^+)$ final molecular ionic states are populated to an extent similar to He I UPS of HCl, (1) a non-Franck−Condon feature with a long and weak vibrational progression was found beyond $v' = 2$ for the $HCl^+(X\ ^2\Pi_i)$ state, indicating slight bond stretching in HCl upon He*(2^3S) atom approach and (2) in both the He*(2^1S) + HCl and HCl*(2^3S) + HCl spectra, the formation of Cl^+ ions was found: energy transfer to repulsive HCl** Rydberg states, dissociating to H(1s), and auto-ionizing Cl** ($^1D_2$ *nl*) atoms leading to $Cl^+(^3P_{2,1})$ ions. By utilizing a theoretical approach, Someda et al.[18] investigated dissociative excitations of HCl in collision with He*(2^3S) by using an SCF−CI calculation of the potential energy hypersurfaces relevant to He*(2^3S) + HCl(X) → He(1^1S) + Cl(^{2}P) + H*($n > 2$). They discussed the mechanism of formation of doubly excited HCl** Rydberg states produced by mixing of a charge-transfer configuration.

Electron kinetic energy (E_e) and collision energy (E_c) resolved two-dimensional (2D) PIES has been used to obtain information about anisotropic interaction potentials around the molecule and also dynamics of particles on the potential energy surface.[19,20] Therefore, Penning ionization probability depends not only on the anisotropic electron distribution of the target molecular orbital (MO) but also on anisotropic interactions between the colliding particles. The cross section may either increase or decrease with increasing the collision energy of the reactants depending on the characteristics of interaction. The positive dependence of the collision energy implies that the interaction is repulsive, whereas the negative dependence indicates an attractive interaction. Thus, it would be very desirable to perform a collision-energy-resolved PIES experiment for a more detailed understanding of the reaction of He*(2^3S) with HCl, because the Penning ionization and the formation of Rydberg states would be influenced by the mutual orientation and collision dynamics of the colliding particles and be different from each other.

Although theoretical approaches are very helpful to elucidate the reaction dynamics, theoretical studies on Penning systems for molecular targets have been limited to a few such as H_2,[21−23] N_2,[24] and H_2O.[25,26] The collision dynamics for the reaction of He*(2^3S) with H_2 has been investigated by the infinite order sudden (IOS),[21,27] close-coupling,[28,29] and the classical trajectory method.[30−32] For the He*(2^3S) + N_2 system, the collision energy dependence obtained by trajectory calculations based on the ab initio potential energy surface with various approximations seems to be in better agreement with the experiment than by the IOS approximation.[24,33] Ogawa and Ohno have reported classical trajectory calculations of the Penning ionization processes based on an ab initio model potential and an overlap

* To whom correspondence should be addressed.
† Present address: Institute for Molecular Science, 38 Nishigonaka, Myodaiji, Okazaki 444-8585, Japan.

10.1021/jp0143793 CCC: $22.00
Published on Web 03/23/2002

approximation for the ionization width for He*(2^3S) with N_2 and CH_3CN.[34,35] Calculated collision energy dependence of the partial ionization cross sections (CEDPICS) qualitatively agreed with the experimental results. Very recently, 2D-PIES has been evaluated by trajectory calculations based on chemical potential surfaces of both entrance and exit channels.[36,37] These studies demonstrated that Li atom usage instead of He*(2^3S) atoms for evaluating interaction potentials and the overlap approximation for trajectory calculations give satisfactory agreement with the experimental results.

In the present paper, we report a collision-energy-resolved PIES study of HCl with the He*(2^3S) atom. CEDPICS has been utilized to obtain information about the anisotropic interaction potential between the colliding particles as well as to discuss the nature of the Rydberg states potential energy surface leading to autoionizing Cl** atoms. Furthermore, classical trajectory calculations have been performed in order to get a deeper insight into the collision dynamics and also to assist the experimental findings.

II. Experimental Section

High purity HCl gas was commercially purchased and used without further purification. The experimental apparatus for measurements of He*(2^3S) PIES and He I UPS has been reported previously.[38−41] Briefly, a metastable He*(2^1S,2^3S) beam was generated by a discharge, and the He*(2^1S) component was optically removed by a helium discharge lamp. He I UPS was measured by He I resonance photons (584 Å, 21.22 eV) produced by a discharge in pure helium gas. Kinetic energy of ejected electrons was measured by a hemispherical electrostatic deflection type analyzer using an electron collection angle 90° to the incident He* and photon beam for PIES and UPS, respectively. We estimate the energy resolution of the electron energy analyzer to be 60 meV from the full width at the half-maximum (fwhm) of the $Ar^+(^2P_{3/2})$ peak in the He I UPS. The observed PIES and UPS were calibrated by the transmission efficiency curve of the electron analyzer, which was alternatively determined by comparing our UPS data of several molecules with those by Gardner and Samson[42] and Kimura et al.[43] Calibration of the electron energy scale was made by reference to the lowest ionic state of N_2 mixed with the sample molecule in He I UPS ($E_e = 5.639$ eV)[44] and He*(2^3S) PIES ($E_e = 4.292$ eV).[10,45]

In the collision-energy-resolved experiments, 2D-PIES, the metastable atom beam was modulated by a pseudorandom chopper rotating about 400 Hz and introduced into the reaction cell located about 500 mm downstream from the chopper disk with keeping constant sample pressure.[19,20] The resolution of the electron analyzer was lowered to 250 meV in order to gain higher electron counting rates. Kinetic electron energies were scanned by 35 meV steps. The 2D Penning ionization data as functions of both E_e and t were converted by Hadamard transformation in which time dependent signals were cross-correlated with the complementary slit sequence of the pseudo-random chopper, and then the velocity dependence of the electron signals was obtained. Velocity distribution of the metastable He* beam, $I_{He^*}(v_{He^*})$, was determined by measuring the intensity of the secondary emitted electrons from the inserted stainless plate. The 2D Penning ionization cross section $\sigma(E_e,v_r)$ was obtained with normalization by the velocity distribution of the He* beam, where v_r is the velocity of the metastable atoms average over the velocity of the HCl molecule. Finally, $\sigma(E_e,v_r)$ is converted to $\sigma(E_e,E_c)$ such as functions of E_e and E_c, where E_c is collision energy of the colliding particles.

III. Calculations

Interaction potential energies between He*(2^3S) and HCl in various directions and distances were calculated on the basis of the well-known resemblance between He*(2^3S) and Li(2^2S);[46] the shape of the velocity dependence of the total scattering cross section of He*(2^3S) by He, Ar, and Kr is very similar to that of Li, and the location of the interaction potential well and its depth are similar for He*(2^3S) and Li with various targets.[47−50] Recently, a precise estimate of the similarity[51] has been made for atomic targets; the well depths for the Li + Y (Y = H, Li, Na, K, Hg) systems were found to be 1.1∼1.2 times larger than those for He*(2^3S) + Y. Because of these findings and the difficulties associated with the calculation of excited states, Li was used in this study in place of He*(2^3S). Thus, the interaction potential HCl−Li(2^2S), $V^*(R,\theta)$ (where R and θ are the distance between Li atoms and X (center of mass of the molecule) and Li-X-Cl angle), was calculated by moving the Li atom and keeping the molecular geometries fixed. For calculating the interaction potential, a quadratic configuration interaction calculation including single and double substitutions with a triple contribution (QCISD(T)) with standard 6-311++G** basis set was used. All of the calculations in this study were performed with the Gaussian 98 quantum chemistry program.[52] The ionization potentials for the HCl were also calculated by using the outer valence Green's function (OVGF) method[53,54] as incorporated in Gaussian 98.

Trajectory calculations for ionization of HCl were performed on a three-dimensional potential energy surface obtained by the QCISD(T)/6-311++G** at more than 900 points. Ionization width was evaluated on the following simplifications; when the angular distribution of the ejected electrons is neglected and when the fact that the He 2s orbital and the continuum orbitals are too diffuse compared to the He 1s and ionized orbitals is taken into account, the positional dependence of the ionization width Γ is mainly governed by the more compact 1s and ionized orbitals. The ionization widths for each ionic states $\Gamma^{(i)}$, therefore, are represented by

$$\Gamma^{(i)} = K|\langle\Phi_i|\Psi_{1s}\rangle|^2 \quad (1)$$

where K is a constant, and Φ_i and Ψ_{1s} are the ionized MO and He 1s orbital, respectively. The impact parameter b was set randomly from 0 to 8 Å for 10 000 trajectories at each collision energy. As the rotational period is not long compared to the collision time, rotational motion during the collision event has been taken into account. The orientation of the HCl was randomly generated, and the initial rotational distribution of the molecule was assumed by Boltzmann distribution at 300 K. The partial ionization cross section $\sigma^{(i)}$ was obtained from ionization probability $P^{(i)}$ with a weight of $2\pi b\ db$

$$\sigma^{(i)} = 2\pi\int bP^{(i)}\ db \quad (2)$$

Details of the trajectory calculations were reported in previous papers.[34,35] The K constant (8.0×10^5) was determined in an iterative way to reproduce experimentally obtained total ionization cross section.

IV. Results

Figure 1 shows the He I UPS and He*(2^3S) PIES of the HCl molecule. The electron energy scale for PIES is shifted relative to that of UPS by the excitation energy difference between He I photons (21.22 eV) and He*(2^3S) (19.82 eV), namely, 1.40 eV.

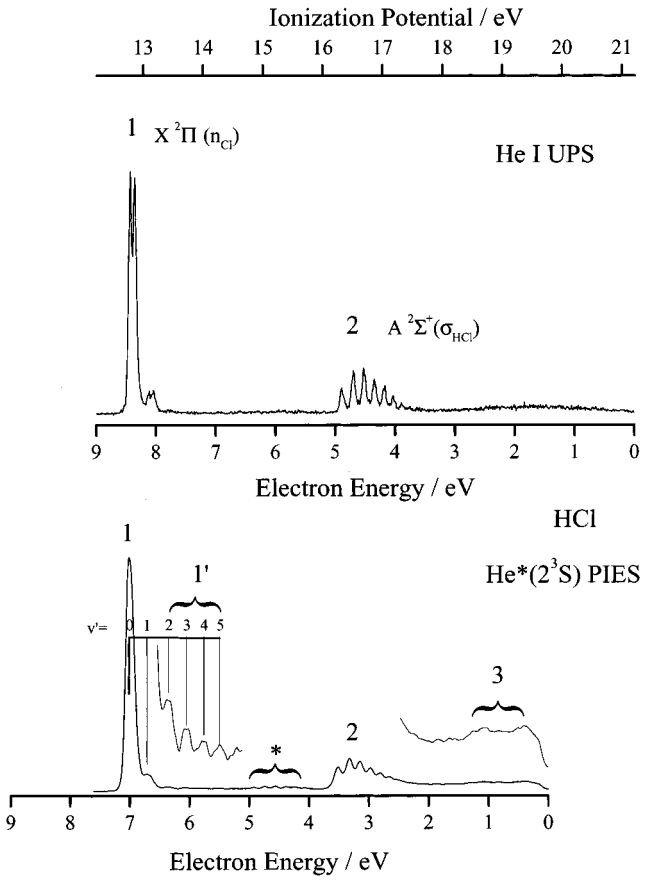

Figure 1. He I UPS and He*(2^{3}S) PIES of HCl. The asterisk is the He I UPS of the A state signal because of the small amount of He I photons accompanied with the He*(2^{3}S) beam.

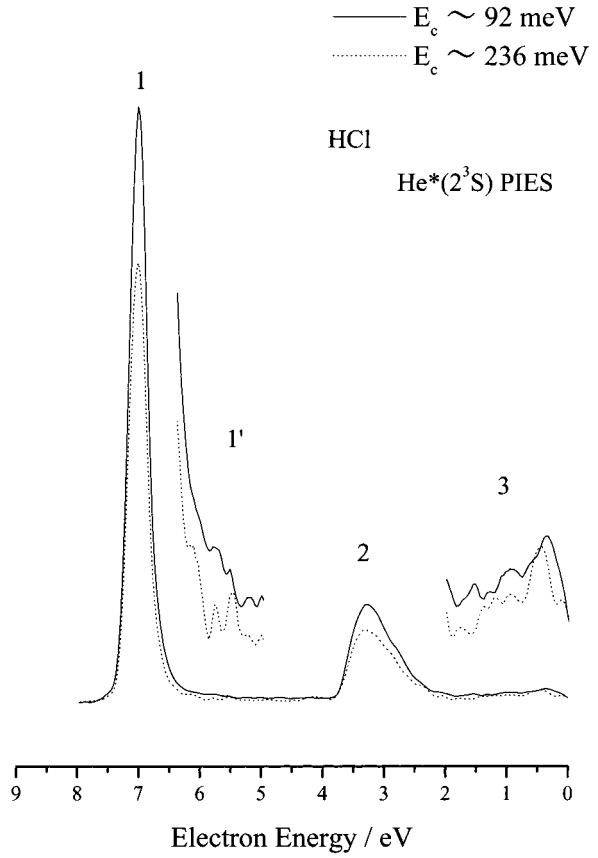

Figure 2. Collision-energy-resolved PIES of HCl with the He*(2^{3}S) atom.

Figure 2 shows the collision-energy-resolved PIES (CERPIES) obtained from the 2D spectra of the HCl molecule. The "hot" spectrum at the higher collision energy (ca. 236 meV) is shown by a dashed curve, and the "cold" one at the lower collision energy (ca. 92 meV) is shown by a solid curve.

Figure 3 shows the log σ versus log E_c plots of CEDPICS in the collision energy range of 90−300 meV for the HCl molecule. The CEDPICS was obtained from the 2D-PIES $\sigma(E_e,E_c)$ within an appropriate range of E_e; band 1 (fwhm of the band), band 1′ (6.6−5.5 eV), band 2 (3.6−2.8 eV), and band 3 (1.5−0.2 eV). Experimental values are plotted by circles. The calculated results for bands 1 and 2 based on the model potential and the overlap approximation for the ionization probabilities are shown by solid lines. The experimental cross sections obtained by the 2D-PIES experiment are normalized to a value of 53 Å^2 for total ionization cross section at E_c = 236 meV estimated by the calculation. In the present calculation, the proportionality constant K in eq 1 is determined in order to reproduce the reported total ionization cross section (62 Å^2 at E_c = 40 meV).[55] It is noted that the reported cross section above is the total quenching cross section of He* atom with HCl, and the branching fraction of Penning ionization over the quenching cross section was separately reported to be 1.00 ± 0.20.[56] Electron density maps with van der Waals surfaces[57] (r_H = 1.2 Å, r_{Cl} = 1.8 Å) are also shown in the figures in order to grasp the effective access direction of He*. The calculated electron density maps for n_{Cl} and σ_{HCl} orbitals are shown on a molecular plane.

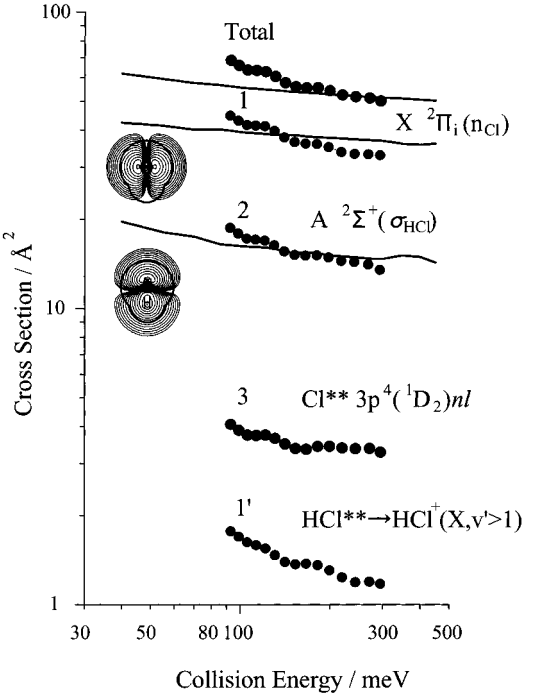

Figure 3. Collision energy dependence of the total and partial ionization cross sections for HCl/He*(2^{3}S). The observed data are plotted by circles. Calculated curves based on the model potential are shown by solid lines. The curves for the total, X $^2\Pi_i$, and A $^2\Sigma^+$ are shown successively from the top. The contour plots show electron density maps for respective MOs.

Figure 4 shows the calculated interaction potential energy curves between ground-state Li atom and the HCl molecule. The potential energies are shown as functions of the distance R and angle θ. Calculations are done at the QCISD(T)/6-311++G** level of theory.

TABLE 1: Band Assignment, Normalized Relative Vibrational Population ($P(v')$), UPS Ionization Potentials (IP/eV), Peak Energy Shifts (ΔE/meV), and Slope Parameters (m) of HCl

band	v'	$P(v')$ in UPS	$P(v')$ in PIES	$P(v')$ FCF[a]	UPS IP_{obsd}/ eV	IP_{OVGF}/ eV (pole strength)	orbital character	ΔE/ meV	m
1	0	100	100	100	12.80	12.33(0.94)	X $^2\Pi_i(n_{Cl})$	-30 ± 10	-0.29 ± 0.02
	1	8.6 ± 0.6	4.1 ± 1.0	7.1				-35 ± 15	
(1′)	2	1.2 ± 1.0	0.68 ± 0.2	0.5				-	-0.38 ± 0.03
	3	-	0.32 ± 0.2					-	
	4	-	0.22 ± 0.2					-	
	5	-	0.19 ± 0.2					-	
2	0	60 ± 3	79 ± 6	63.3	16.28	16.56(0.93)	A $^2\Sigma^+(\sigma_{HCl})$	-7 ± 10	-0.24 ± 0.02
	1	100	100	100				-7 ± 10	
	2	96 ± 3	82 ± 7	94.3				$+6 \pm 10$	
	3	73 ± 3	50 ± 7	69.8				$+13 \pm 10$	
	4	50 ± 4	39 ± 7	45.2				$+3 \pm 10$	
	5	28 ± 4	23 ± 8	27.1				$+1 \pm 10$	
	6	16 ± 5	-	15.5				-	
	7	8 ± 5	-						
3					18.4 ∼			-	-0.15 ± 0.01

[a] D. L. Albritton, results cited in refs 6 and 11.

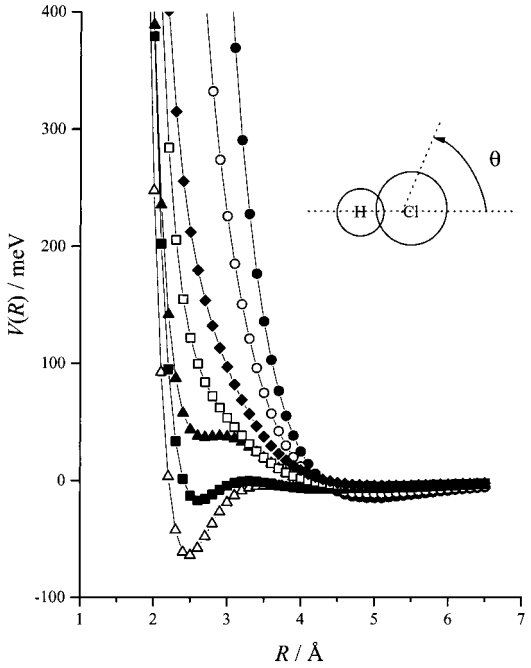

Figure 4. Entrance potentials for directions of 0°(●), 30°(○), 60°(▲), 90°(△), 120°(■), 150°(□), and 180°(◆) with respect to the H−Cl axis obtained by the QCISD(T)/6-311++G** calculation. Note that the origin of the angle is a center-of-mass of the HCl molecule.

Table 1 summarizes experimentally observed, normalized relative population of each electronic state ($P(v')$), calculated IPs, experimental peak energy shifts (ΔE), slope parameters of CEDPICS (m), and the assignment of the bands. Slope parameters are obtained from the log σ vs log E_c plots in a collision energy range for 90−300 meV by a least-squares method. Vertical IPs are determined from He I UPS. The peak energy shifts are obtained as the difference between the peak position (E_{PIES}; electron energy scale) and the "nominal" value (E_0 = difference between metastable excitation energy and sample IP): $\Delta E = E_{PIES} - E_0$. Errors in m values are estimated by several measurements. Tables 2 and 3 are comparison with the past studies.[6,7,9−11]

V. Discussion

A. General Feature of PIES. PIES of HCl molecule with the He*(2^3S) atom is shown in Figure 1 together with UPS. PIES studies have been reported by several authors.[6−11] The present result is very close to the past study of Yencha et al.,[11] whereas the average collision energy of the present study (∼160 meV) shown in Figure 1 is larger than the one (60 meV) in ref 11. Observed features in the present study can be summarized as follows: (1) Band intensity for the X state (n_{Cl} orbital) was enhanced with respect to the one for the A state. (2) Non-Franck−Condon behavior was found in the excited vibrational levels ($v' > 1$) of the X state. Namely, the formation of the X state is characterized by an intense $v' = 0$ band followed by much weaker vibrational structure up to $v' = 5$. (3) Steplike-rise and followed continuum broad band was found for lower electron kinetic energy region labeled as band 3.

TABLE 2: Peak Energy Shift (ΔE/meV) of the Vibrational Ground State ($v' = 0$)

	HCl^+ electronic state	
reference	X $^2\Pi_i$	A $^2\Sigma^+$
7	-50 ± 5	-15 ± 5
9	-76 ± 20	-77 ± 20
10	-28 ± 6	-3 ± 8
11	-28 ± 2	$+2 \pm 4$
this work	-30 ± 10	-7 ± 10

TABLE 3: Relative Population of Electronic States of HCl^+ Measured at 90° to the Incident He* Beam

	HCl^+ electronic state	
reference	X $^2\Pi_i$	A $^2\Sigma^+$
6	1.00	0.50 ± 0.04
10	1.00	0.51 ± 0.03
11	1.00	0.53 ± 0.02
this work	1.00	0.51 ± 0.04[a]

[a] The branching ratio was obtained from Figure 1. The average collision energy was measured to be 160 meV.

B. CEDPICS of X and A States. The Penning ionization process can be explained by the electron exchange model where an electron of the target molecular orbital (MO) is transferred into the inner vacant 1s orbital of the He* atom, which subsequently ejects the external electron in 2s orbital.[58] Then the mutual overlap of related orbitals for the electron exchange plays an important role.[2,59] The first finding can be ascribed that the large electron density of the n_{Cl} orbital shows stronger attractive interaction than corresponding region of the σ_{HCl} orbital. Furthermore, attractive interaction is expected to bring larger overlap than repulsive interaction under the investigated collision energy range. Partial ionization cross sections of bands 1 and 2 are well reproduced by the trajectory calculations.

Namely, the observed branching ratio of A to X state is well reproduced by the trajectory calculation in the investigated collision energy range as shown in Figure 3. The branching fraction between X and A states summarized in Table 3 agrees with the reported one despite different collision energy, for example 60 meV for ref 11. This fact suggests that the collision energy dependence of the partial ionization cross sections for these states are not significantly different from each other. The collision energy dependence of bands 1 and 2 shows a similar negative nature both in experiment and calculations as shown in Figure 3 in accord with the above prediction.

Although the collision energy dependence of the total ionization cross section, namely, $\sigma_{TI} \propto E_c^{-0.58}$, over the relative collision energy range 5−334 meV, in the He*(2^3S) and HCl Penning ionization has been reported by Parr et al.,[60] a direct correspondence between the measurements may not be necessary. Whereas Parr et al.[60] measured the total ionization cross section of the He*(2^3S) with the HCl molecule by detecting positive ions, we detected the ejected electrons whose kinetic energy was analyzed. However, the difference of the slope parameter seems to be too much to be addressed only to the difference of detecting species. Both experimental approaches to measure the collision energy dependence of the ionization cross section have been well established,[19,60] whereas the detection of positive ions without mass selection should perform with great care in order to eliminate any contribution from impurities. It should be mentioned that the beam characteristics of the HCl gas between these experiments are different from each other: we introduced HCl gas at 300 K, whereas Parr et al.[60] used it at 160 K. Therefore the difference may arise from the different beam character. At 160 K, even in the effusive beam condition, the HCl dimer can be formed.[61] It seems that the result of Parr et al.[60] contains a certain contribution from the dimer, because a cross section of the cluster may be a couple of magnitudes larger compared to that of the monomer as found in the other reaction system.[62] On the contrary, present results purely arise from the reaction of the HCl monomer with the He* atom.

Negative CEDPICS of bands 1 and 2 indicate the existence of an attractive interaction potential around the molecule. Negative peak energy shifts were consistently observed for bands 1 and 2, whereas band 2 shows a very small peak energy shift as summarized in Tables 1 and 2. Obtained peak energy shifts are in good agreement with past studies. Model potential calculation of the present system shows attractive interaction for the side way approach of the He* atom toward a HCl molecule (n_{Cl} orbital region) and repulsive one for the collinear direction along the H−Cl bond axis (σ_{HCl} orbital region). On the basis of a zero impact parameter model, it may be puzzling that both the experimental and calculated CEDPICSs for band 2 show negative character, because the electron density distribution for the corresponding molecular orbital has major contribution around the repulsive interaction region. It has been fairly well recognized that the zero impact parameter picture is too simple to figure out the true nature of reaction dynamics. The negative feature of band 2 is an indication that this band contains a certain contribution related to molecules imposed attractive interaction at the collision event. It is easily recognized that for the trajectories having larger impact parameters the glancing collisions of the He* atoms with the HCl molecule along its molecular axis play a dominant role, because the trajectories for smaller impact parameters relevant to the collinear approach to the bond axis only yield a small ionization cross section. It is noted to mention that, although the trajectories of the He* atom was mostly influenced by the attractive interaction around the Cl atom sideways to the molecular axis, the ionization point is the exterior region of the σ_{HCl} orbital. This argument is inconsistent with both the observed small peak energy shift and the negative character in CEDPICS of this band. The experimentally obtained absolute value of the negative slope in CEDPICS for band 1 is slightly larger than the one for band 2, whereas the calculation results indicate the opposite way. This disagreement suggests that the reported cross section may be rather large, because the larger cross section implies the large contribution from the reaction at larger impact parameter. In fact, Bush et al.[55] estimated uncertainties about 30% for their reported ionization cross section. Furthermore, the nonionization channel may be involved within the reported uncertainty of 20% to the total quenching cross section as reported in ref 56. It is noted that a smaller K constant in eq 1, which leads to a smaller total ionization cross section, reproduces the larger attractive effect for band 1 than for band 2. Experimental results indicate that ionization around the n_{Cl} orbital region has been influenced by a larger attractive effect than the σ_{HCl} orbital region, because the n_{Cl} orbital has larger electron density around the attractive region. It is also noted that the experimental absolute slope values in CEDPICS both for bands 1 and 2 are larger than the ones obtained by the calculations. The difference between the experiment and calculation can be partially explained by the underestimation of the attractive well (∼64 meV at $R = 2.5$ Å and $\theta = 90°$) for the present QCISD calculation. In fact, Yencha et al.[11] pointed out that the depth of the attractive potential well (∼84 meV for X state estimated from the edge shift) was larger because of the shallow potential well (∼20 meV) for the exit channels. In addition, theoretical calculations suggest that the HCl bond stretch because of the approach of the He* atom is a slightly larger attractive effect as discussed later. Therefore, larger absolute values of CEDPICS for bands 1 and 2 in the experiment can be rationalized to the above arguments. Here, we have to mention that an inclusion of this stretching effect in the trajectory calculation has not been performed because of the difficulty in estimating the magnitude of bond stretching at various conditions: impact parameter, collision energy, and orientation of the reagents.

C. Rydberg HCl States.** Arguments for a sizable entrance channel attraction above might be partially responsible for the significant deviations of the vibrational distribution from the Franck−Condon expectation, in the sense that HCl bond stretching occurs upon approach of the He* atom, finding (2). However, a major potion of the spectrum, namely, the vibrational population of HCl^+(X, $v' = 0,1$) and HCl^+(A,$v' = 0-4$), is almost identical to the He I UPS. Thus, it is natural that a long progression of vibrational bands in the X state can be ascribed to a different origin from the normal Penning ionization mechanism. As suggested by Yencha et al.,[11] the origin of vibrational progression $v' > 1$ should be related to the formation of an autoionizing superexcited state of HCl close to the excitation energy of the He*(2^3S) atom. A similar superexcited state was also found in Ne I UPS, where excitation up to $v' = 13$ in HCl^+(X) was found and attributed to an autoionizing transition originating from unknown superexcited state of HCl that is energy-resonant with each of the Ne I lines (16.848 and 16.671 eV).[63] The absolute slope value of the CEDPICS for the corresponding region labeled as band 1′ is larger than that of any other bands, which indicates the strongest attractive effect. Indeed, Palmieri et al.[64] have presented an ab initio calculated potential energy surface of the Li + HCl system for a larger number of molecular geometries, showing that bond

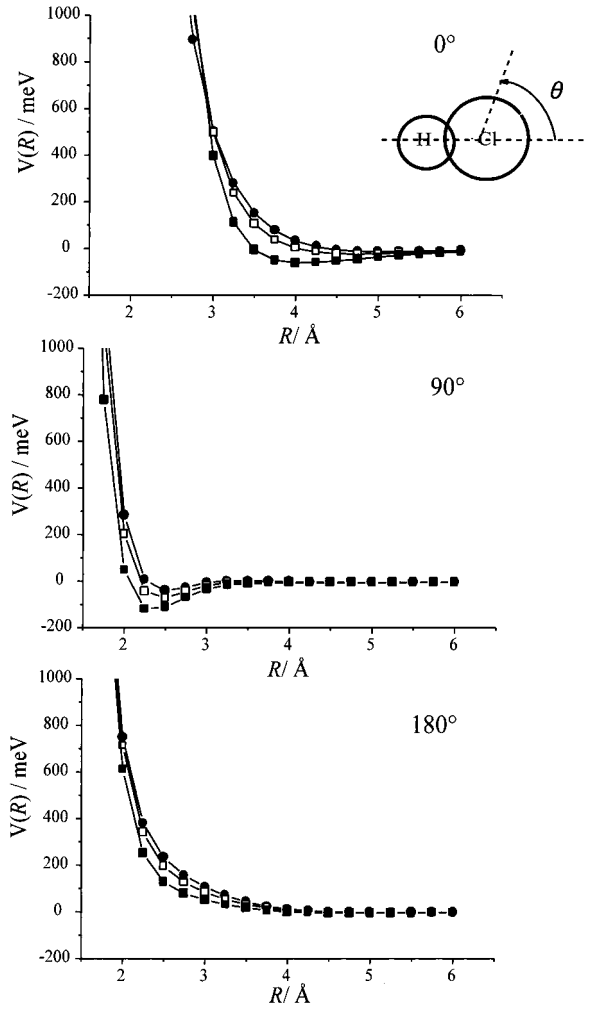

Figure 5. Entrance potentials for directions of 0°, 90°, and 180° with respect to the H−Cl axis at a few HCl bond distances obtained by the MP2/6-311++G** calculations. (●) HCl bond distance r is 1.247 Å, (□) r = 1.35 Å, and (■) r = 1.45 Å, which correspond to the bond lengths of HCl in the v = 0, 1, and 2 states, respectively. Note that the origin of the angle is a center-of-mass of the HCl molecule.

stretching in the HCl molecule by Li approach from any direction is a quite important effect. Independently, we have performed similar calculation at a few HCl bond distances by using the second-order Møller−Plesset perturbation theory (MP2) with 6-311++G** calculations as shown in Figure 5 and found equivalent results. Namely, attractive interaction becomes larger with the increment of the bond distance. These findings should be closely related to the indication of the largest attractive effect for band 1′, because avoided crossing between the He*−HCl and He−HCl** surfaces should occur at the longer HCl bond distance than the HCl molecule in the ground state. Furthermore, Yencha et al.[11] roughly estimated the upper limit of the well depth of this broad band to be 410 meV by the difference between the nominal energy E_0 and the lowest emitted electron energy taken as the 10% point of the peak maximum intensity on the low energy tail. This is also consistent with our conclusion that the attractive interaction becomes larger with the increment of the bond distance of HCl.

Yencha et al.[11] clearly observed the atomic structured region superimposed on an underlying broad band below an electron energy of 1.42 eV. They identified the four series ns, np, nd′, and nd with the core configuration Cl $3p^4(^1D_2)$, autoionizing the Cl** atom to the two final states Cl^+ $3p^4(^3P_2)$ and Cl^+ $3p^4(^3P_1)$. Moreover, the production mechanism leading to the formation of the autoionizing Cl** atoms was proposed with excitation transfer

$$He(2^3S) + HCl \rightarrow He + HCl^{**}$$
$$HCl^{**} \rightarrow H + Cl^{**}$$

which finally results in autoionization

$$Cl^{**} \rightarrow Cl^+ + e^-$$

to produce the sharp electron peaks as well as the underlying broad continuum. Similarly, we observed a steplike-rise at 1.4 eV followed by a structureless band (feature 3). It is important to mention that the resolution (60 meV) of our spectrometer was lower than that (17−18 meV) of Yencha et al.[11] Thus, the lack of observation of atomic structures can be attributed to the relatively low resolution in combination with the weak intensity of these features. As mentioned before, the observation of collision-energy-dependent cross sections provides valuable information about the interaction. The absolute slope value of CEDPICS for this band is the smallest among the bands observed, which indicates either weak attractive or repulsive potential character around the avoided crossing between He*−HCl and He−HCl** potential energy surfaces. The knowledge of the He*−HCl and He−HCl** potential energy surfaces would be very helpful. Someda et al.[18] calculated these potential energy surfaces by a SCF−CI method in order to investigate the dissociative excitation of HCl in collision with the He*(2^3S) atom. The calculated potential energy curves were found to be anisotropic with respect to the angle of approach θ of the He* atom. On the basis of the calculated potential energy surfaces, they proposed the dissociation mechanism into the H and Cl atoms: when the He*(2^3S) approaches HCl, the motion of the zero-point vibration of HCl causes the transition from the He*(2^3S) + HCl to He + HCl** through the avoided crossings. They focused their discussion on the thermal collision accessible by two states, 2 $^2\Sigma^+$-4s and 1 $^4\Pi$-4p, and concluded that the HCl**(2 $^2\Sigma^+$-4s) could be the dominant final channel. It should be mentioned that the HCl**(2 $^2\Sigma^+$-4s) state is not directory correlated to the $Cl^+(^3P_{2,1})$ but to $Cl^+(^1D_2)$ at the dissociation limit. On the other hand, Yencha et al.[11] suggested that the HCl-(1 $^4\Pi$-4p) state might be a candidate for one of the precursor states of the Cl** $3p^4(^1D_2)nl$ states, assuming that the HCl**(1 $^4\Pi$-4p) state would decay into lowering HCl**(1 $^2\Delta$-nl) states by curve crossing, because the HCl**(1 $^2\Delta$-nl) states is energy resonant with He*(2^3S) and dissociating into the H + Cl** $3p^4(^1D_2)$ 4s, which correlates to the $Cl^+(^3P_{2,1})$ formation. The calculated potential curves by Someda et al.[18] indicated that the avoided crossing between the He + HCl**(1 $^4\Pi$-4p) and the He*(2^3S) + HCl only appears in the collinear approach of the He* atom on the Cl end of HCl. In this respect, the ionization event for band 3 should be governed by the repulsive interaction around the Cl atom. This is consistent with the smallest absolute slope value of CEDPICS for band 3, because the Cl end-on approach of the He* atom to the HCl shows repulsive interaction as shown in Figure 4. This finding may support the formation mechanism of Cl**($^1D_2$) proposed by Yencha et al.[11]

VI. Conclusion

We have measured the two-dimensional PIES of the HCl molecule with the He*(2^3S) atom. In addition, we have performed classical trajectory calculations of the reactants on the model potential energy surface obtained by ab initio molecular orbital calculations. CEDPICS shows negative char-

acter, which implies the importance of attractive interaction around the molecule. By combining results of the CEDPICS both in experiment and calculation, it was found that the attractive interaction around the side of the HCl molecular axis takes a crucial role to produce $HCl^+(X\ ^2\Pi_i,\ v' = 0,1)$ and $HCl^+(A\ ^2\Sigma^+)$. Furthermore, reaction pathways for generating the Cl** autoionizing atoms were dominant for the collinear approach of the He* atom on the Cl end of HCl molecule.

Acknowledgment. This work has been partially supported by a Grant in Aid for Scientific Research from the Japanese Ministry of Education, Science, and Culture. One of the authors (K.I) thanks the Japan Society for the Promotion of Science (JSPS) for a JSPS Research Fellowship.

References and Notes

(1) Penning, F. M. *Naturwissenschaften* **1927**, *15*, 818.
(2) (a) Ohno, K.; Mutoh, H.; Harada, Y. *J. Am. Chem. Soc*. **1983**, *105*, 4555. (b) Ohno, K.; Harada, Y. In *Theoretical Models of Chemical Bonding*; Maksić, Z. B., Ed.; Springer-Verlag: Berlin, Germany, 1991; p 199.
(3) Niehaus, A. *Adv. Chem. Phys*. **1981**, *45*, 399.
(4) Yencha, A. J. In *Electron Spectroscopy: Theory, Technique, and Applications*; Brundle, C. R., Baker, A. D., Eds.; Academic: New York, 1984; Vol. 5.
(5) Siska, P. E. *Rev. Mod. Phys*. **1993**, *65*, 337.
(6) Hotop, H.; Hüber, G.; Kaufhold, L. *Int. J. Mass. Spectrom. Ion Phys*. **1975**, *17*, 163.
(7) Cermák, V. *J. Electron Spectrosc. Relat. Phenom*. **1976**, *9*, 419.
(8) Cermák, V. *J. Electron Spectrosc. Relat. Phenom*. **1976**, *8*, 325.
(9) Brion, C. E.; Crowley, P. *J. Electron Spectrosc. Relat. Phenom*. **1977**, *11*, 399.
(10) Hotop, H.; Hüber, G. *J. Electron Spectrosc. Relat. Phenom*. **1977**, *11*, 101.
(11) Yencha, A. J.; Ganz, J.; Ruf, M.-W.; Hotop, H. *Z. Phys. D* **1989**, *14*, 57.
(12) Richardson, W. C.; Setser, D. W.; Albritton, D. L.; Schmeltekopf, A. L. *Chem. Phys. Lett*. **1971**, *12*, 249.
(13) Richardson, W. C.; Setser, D. W. *J. Chem. Phys*. **1973**, *58*, 1809.
(14) de Vries, M. S.; Tyndall, G. W.; Martin, R. M. *J. Chem. Phys*. **1984**, *80*, 1366.
(15) Tsuji, M.; Maier, J. P.; Obase, H.; Nishimura, Y. *Chem. Phys. Lett*. **1986**, *110*, 17.
(16) Obase, H.; Tsuji, M.; Nishimura, Y. *J. Chem. Phys*. **1987**, *87*, 2695.
(17) Simon, W.; Yencha, A. J.; Ruf, M.-W.; Hotop, H. *Z. Phys. D* **1988**, *8*, 71.
(18) Someda, K.; Kosugi, N.; Kondow, T.; Kuchitsu, K. *J. Phys. Chem*. **1989**, *93*, 35.
(19) Ohno, K.; Yamakado, H.; Ogawa, T.; Yamata, T. *J. Chem. Phys*. **1996**, *105*, 7536.
(20) Kishimoto, N.; Aizawa, J.; Yamakado, H.; Ohno, K. *J. Phys. Chem. A* **1997**, *101*, 5038.
(21) Cohen, J. S.; Lane, N. F. *J. Chem. Phys*. **1977**, *66*, 586.
(22) Hickman, A. P.; Isaacson, A. D.; Miller, W. H. *J. Chem. Phys*. **1977**, *66*, 1483.
(23) Isaacson, A. D.; Hickman, A. P.; Miller, W. H. *J. Chem. Phys*. **1977**, *66*, 370.
(24) Ishida, T. *Chem. Phys. Lett*. **1992**, *191*, 1.
(25) Haug, B.; Morgner, H.; Staemmler, V. *J. Phys. B* **1985**, *18*, 259.
(26) Ishida, T. *J. Chem. Phys*. **1995**, *102*, 4169.
(27) Martin, D. W.; Siska, P. E. *J. Chem. Phys*. **1985**, *82*, 2630.
(28) Hickman, A. P.; Isaacson, A. D.; Miller, W. H. *J. Chem. Phys*. **1977**, *66*, 1492.
(29) Martin, D. W.; Siska, P. E. *J. Chem. Phys*. **1989**, *89*, 240.
(30) Preston, R. K.; Cohen, J. S. *J. Chem. Phys*. **1976**, *65*, 1589.
(31) Vojtík, J. *Chem. Phys*. **1996**, *209*, 367.
(32) Vojtík, J.; Kotal, R. *Chem. Phys. Lett*. **1996**, *255*, 251.
(33) Ishida, T.; Horime, K. *J. Chem. Phys*. **1996**, *105*, 5380.
(34) Ogawa, T.; Ohno, K. *J. Chem. Phys*. **1999**, *110*, 3773.
(35) Ogawa, T.; Ohno, K. *J. Phys. Chem. A* **1999**, *103*, 9925.
(36) Ohno, K.; Yamazaki, M.; Kishimoto, N.; Ogawa, T.; Takeshita, K. *Chem. Phys. Lett*. **2000**, *332*, 167.
(37) Yamazaki, M.; Kishimoto, N.; Kurita, M.; Ogawa, T.; Ohno, K.; Takeshita, K. *J. Electron Spectrosc. Relat. Phenom*. **2001**, *114*−*116*, 175.
(38) Takami, T.; Ohno, K. *J. Chem. Phys*. **1992**, *96*, 6523.
(39) Mitsuke, K.; Takami, T.; Ohno, K. *J. Chem. Phys*. **1989**, *91*, 1618.
(40) Ohno, K.; Takami, T.; Mitsuke, K.; Ishida, T. *J. Chem. Phys*. **1991**, *94*, 2675.
(41) Takami, T.; Mitsuke, K.; Ohno, K. *J. Chem. Phys*. **1991**, *95*, 918.
(42) Gardner, J. L.; Samson, J. A. R. *J. Electron Spectrosc. Relat. Phenom*. **1976**, *8*, 469.
(43) Kimura, K.; Katsumata, S.; Achiba, Y.; Yamazaki, T.; Iwata, S. *Handbook of He I Photoelectron Spectra of Fundamental Organic Molecules*; Japan Scientific: Tokyo, 1981.
(44) Turner, D. W.; Baker, C.; Baker, A. D.; Brundle, C. R. *Molecular Photoelectron Spectroscopy*; Wiley: London, 1970.
(45) Yee, D. S. C.; Stewart, W. B.; Mcdowell, C. A.; Brion, C. E. *J. Electron Spectrosc. Relat. Phenom*. **1975**, *7*, 93.
(46) Rothe, E. W.; Neynaber, R. H.; Trujillo, S. M. *J. Chem. Phys*. **1965**, *42*, 3310.
(47) Illenberger, E.; Niehaus, A. *Z. Phys. B*. **1975**, *20*, 33.
(48) Parr, T. P.; Parr, D. M.; Martin, R. M. *J. Chem. Phys*. **1982**, *76*, 316.
(49) Hotop, H. *Radiat. Res*. **1974**, *59*, 379.
(50) Haberland, H.; Lee, Y. T.; Siska, P. E. *Adv. Chem. Phys*. **1981**, *45*, 487.
(51) Hotop, H.; Roth, T. E.; Ruf, M.-W.; Yencha, A. J. *Theor. Chem. Acc*. **1998**, *100*, 36.
(52) Frisch, M. J.; Trucks, G. W.; Schlegel, H. B.; Scuseria, G. E.; Robb, M. A.; Cheeseman, J. R.; Zakrzewski, V. G.; Montgomery, J. A., Jr.; Stratmann, R. E.; Burant, J. C.; Dapprich, S.; Millam, J. M.; Daniels, A. D.; Kudin, K. N.; Strain, M. C.; Farkas, O.; Tomasi, J.; Barone, V.; Cossi, M.; Cammi, R.; Mennucci, B.; Pomelli, C.; Adamo, C.; Clifford, S.; Ochterski, J.; Petersson, G. A.; Ayala, P. Y.; Cui, Q.; Morokuma, K.; Malick, D. K.; Rabuck, A. D.; Raghavachari, K.; Foresman, J. B.; Cioslowski, J.; Ortiz, J. V.; Stefanov, B. B.; Liu, G.; Liashenko, A.; Piskorz, P.; Komaromi, I.; Gomperts, R.; Martin, R. L.; Fox, D. J.; Keith, T.; Al-Laham, M. A.; Peng, C. Y.; Nanayakkara, A.; Gonzalez, C.; Challacombe, M.; Gill, P. M. W.; Johnson, B. G.; Chen, W.; Wong, M. W.; Andres, J. L.; Head-Gordon, M.; Replogle, E. S.; Pople, J. A. *Gaussian 98*; Gaussian, Inc.: Pittsburgh, PA, 1998.
(53) von Niessen, W.; Schirmer, J.; Cederbaum, L. S. *Comput. Phys. Rep*. **1984**, *1*, 57.
(54) (a) Zakrzewski, V. G.; Ortiz, J. V. *Int. J. Quantum Chem. Symp*. **1994**, *28*, 23. (b) Zakrzewski, V. G.; Ortiz, J. V. *Int. J. Quantum Chem*. **1995**, *53*, 583.
(55) Bush, Y. A.; McFarland, M.; Albritton, D. L.; Schmeltekopf, A. L. *J. Chem. Phys*. **1973**, *58*, 4020.
(56) Jones, M. T.; Dreiling, T. D.; Setser, D. W.; McDonald, R. N. *J. Phys. Chem*. **1985**, *89*, 4501.
(57) Pauling, L. *The Nature of the Chemical Bond*; Cornell University: Ithaca, NY, 1960.
(58) Hotop, H.; Niehaus, A. *Z. Phys*. **1969**, *228*, 68.
(59) Ohno, K.; Matsumoto, S.; Harada, Y. *J. Chem. Phys*. **1984**, *81*, 4447.
(60) Parr, T. P.; Hanson-Parr, D.; Martin, R. M. *Int. Conf. Phys. Electron. At. Collisions, 11th* **1979**, 878.
(61) Rank, D. H.; Sitaram, P.; Glickman, W. A.; Wiggins, T. A. *J. Chem. Phys*. **1963**, *39*, 2673.
(62) Hurwitz, Y.; Stern, P. S.; Naaman, R. *J. Chem. Phys*. **1997**, *106*, 2627.
(63) Natalis, P.; Pennetreau, R.; Longton, L.; Collin, J. E. *J. Electron Spectrosc. Relat. Phenom*. **1982**, *27*, 267.
(64) Palmieri, P.; Garcia, E.; Laganá, A. *J. Chem. Phys*. **1988**, *88*, 181.